Monthly Notices
of the
ROYAL ASTRONOMICAL SOCIETY

Mon. Not. R. Astron. Soc. **408,** 293–299 (2010) doi:10.1111/j.1365-2966.2010.17104.x

Longitudinal magnetic tube wave fluxes in stars of low metallicity

Diaa E. Fawzy★
Faculty of Engineering and Computer Sciences, Izmir University of Economics, 35330 Izmir, Turkey

Accepted 2010 May 27. Received 2010 May 26; in original form 2010 February 21

ABSTRACT
A modified theory of turbulence generation is combined with the magnetohydrodynamic equations to numerically compute the wave energies generated at the base of magnetic flux tubes for stars with effective temperatures ranging from $T_{\rm eff} = 3000$ to 7000 K, gravity $\log g = 4.44$ and with different metal abundances: solar, 0.1, 0.01 and 0.001 of solar metallicity. The results show that the effect of metallicity is very important for cool stars ($T_{\rm eff} < 5500$ K). The current numerical approach allows for non-linear waves with large amplitudes and thus the obtained results for time-averaged wave energy fluxes are higher than those obtained by the analytical approach. For hot stars the effect is negligible. The computed energy fluxes are essential for constructing theoretical models of the magnetic chromosphere of low-metallicity stars. The maximum obtained wave energy flux for low-metallicity stars is about 7.3×10^8 erg cm^{-2} s^{-1}.

Key words: MHD – waves – methods: numerical – stars: chromospheres – stars: coronae – stars: magnetic field.

1 INTRODUCTION

Except for rare cases, chromospheres and coronae are outer layers of stars that are not affected by the interstellar medium in which the stars are embedded or influenced by neighbouring stars. The architecture and physics of these layers must therefore be completely dependent on the internal structure of their parental stars. Although the basic physics of the chromospheres and coronae is still not completely understood, it is well known that these outer layers represent environments with a peculiar physics. While there are extended areas on the stellar surfaces devoid of magnetic fields, there are also regions where magnetic fields are bundled into intense flux tubes. Because at a given height their interior is less dense than their surroundings, these tubes are buoyant and thought to be oriented vertically at the stellar surface and to spread with height.

One peculiarity is the fact that the radiation field in the chromospheres depends strongly on direction, leading to a situation where departures from thermodynamic equilibrium (non-local thermodynamic equilibrium effects) are dominant. In addition, due to the low gas density a few scaleheights above the stellar surface, the recombination processes are severely impaired, leading to characteristic overionization effects which are particularly conspicuous in time-dependent processes such as waves.

Another essential ingredient of the peculiar physics of chromospheres and coronae is that they are layers with significant amounts of mechanical heating. This heating either by waves or by the reconnection of magnetic field lines is also poorly understood. What is well known, however, is that the culprit for the generation of both types of mechanical energy is the convection zone and particularly the outermost layers where the convective flows are fastest. These turbulent flows generate waves either directly as in the case of acoustic waves or indirectly by perturbing the magnetic flux tubes.

Fortunately, because the mechanical energy generation takes place below the stellar surface, the problem of modeling and predicting chromospheres and coronae can be split into two parts: first the mechanical energy production, and secondly the construction of models with their peculiar physics (as e.g. Fawzy et al. 2002a). We concentrate here on the mechanical energy production that depends on whether one has a region permeated by magnetic fields or one without fields. For field-free regions where the main heating mechanism is acoustic waves, we have computed the spectra and energy fluxes of these waves for a wide variety of stars of different effective temperatures $T_{\rm eff}$, gravities $\log g$ and metallicities $Z_{\rm m}$ (Ulmschneider, Theurer & Musielak 1996; Ulmschneider et al. 1999). Created by turbulence in the stellar convection zone, some waves propagate under a wide range of angles in outward directions, and due to the rapid density decrease near the stellar surface they steepen into shocks above it. This shock dissipation constitutes the mechanical heating of the outer layers of the star. As the convection zones depend only on three parameters such as $T_{\rm eff}$, gravity g and metallicity $Z_{\rm m}$, the acoustic energy fluxes and therefore non-magnetic chromospheres also depend only on three parameters.

In the magnetic case the turbulent convective flows in the presence of stellar rotation generate magnetic fields. These fields represent stored mechanical energy that by reconnection can be liberated to produce heating. In addition, convective flows perturb magnetic flux tubes and generate various types of magnetic tube waves such as longitudinal, transverse (kink) and torsional waves. For transverse waves (Huang, Musielak & Ulmschneider 1995) and longitudinal

★E-mail: diaa.gadelmavla@ieu.edu.tr

waves (Ulmschneider, Musielak & Fawzy 2001, hereafter Paper I), energy fluxes have been computed for cases of stars with different $T_{\rm eff}$, $\log g$ and solar metal abundance, $Z_{\rm m0}$. Since for the generation of magnetic fields in stellar convection zones stellar rotation is an additional parameter, the mechanical magnetic energy generation and consequently chromospheres and coronae are expected to depend on four parameters.

Since a dynamo theory that predicts the magnetic flux on a star given these four parameters is presently missing, it has been discussed when constructing magnetic chromosphere models produced by longitudinal magnetic wave heating (Fawzy et al. 2002a,b,c) that the stellar rotation can be replaced by specifying a magnetic filling factor f, i.e. the ratio of the area covered by magnetic flux to the total stellar surface area. Assuming that most of the area permeated by magnetic flux of a star (sunspots constitute only a small fraction of this flux) is in the form of flux tubes with roughly similar individual size, the determination of magnetic wave energy in stars of different rotation rates can be reduced to a computation of the wave flux from a single flux tube multiplied by the number of flux tubes per area given by the filling factor and ultimately by the rotation rate.

As was the case for Paper I, we thus concentrate on the computation of longitudinal waves in a single magnetic flux tube sitting vertically in the stellar surface being perturbed by the turbulent convective motions that are largest right below that surface. Different from Paper I is now that in stars with lower metallicity the opacity is reduced for cool stars where metals are an important opacity source, and consequently the stellar surface where the continuum optical depth is 1 occurs in regions of higher density where the maximum convective velocities are much smaller.

The influence of the metallicity on wave generation has been first investigated analytically by Ulmschneider et al. (1999) for acoustic waves and later by Musielak, Rosner & Ulmschneider (2002) for magnetic flux tube waves. In the later approaches, the turbulence has been simulated by two components: a spatial component is described by an extended Kolmogrov turbulent energy spectrum and a temporal component represented by a modified Gaussian frequency factor.

The main goal of this paper is to extend previous work by taking into account non-linear effects and thus allowing for waves with large amplitudes in stars of low metal abundances. The computed energy fluxes are essential for constructing realistic magnetic models of chromospheres of low-metallicity stars. A brief description of the method of computation is given in Section 2, the results and discussion are presented in Section 3 and final conclusions are given in Section 4.

2 METHOD OF COMPUTATION

We now briefly summarize the numerical approach used in the current computations. For details we refer to Paper I.

2.1 Stellar magnetic flux tube models

Since, even for the Sun, observation of stellar magnetic flux tubes is difficult due to their small size of below a scaleheight, we assume that we can model these tubes using the *thin flux tube approximation*. 2D modelling of magnetic flux tubes by Hassan et al. (2003) has shown that this approach gives accurate results as long as one does not go more than a few scaleheights above the stellar surface, which in our case is certainly satisfied. We extend the commonly accepted concept of solar magnetic flux tubes (e.g. Stenflo 1978; Solanki 1993) to stellar flux tubes. A stellar magnetic flux tube at the stellar surface is assumed to have a diameter roughly equal to the local scaleheight. For the Sun, the magnetic flux tubes at the surface have field strengths of the order of $B_{\rm o} = 1500$ G (e.g. Solanki 1993). When taking $p_{\rm e} = 1.17 \times 10^5$ dyn cm^{-2} from model C of Vernazza, Avrett & Loeser (1981) at the height $z = 0$ where $\tau_{5000} = 1$, one gets an equipartition field strength ($B_{\rm eq}^2/8\pi = p_{\rm e}$) of $B_{\rm eq} = 1716$ G. We thus find a ratio $B/B_{\rm eq} = 0.875$ and consider it as typical for both solar and stellar flux tubes. We keep this ratio constant for all our computations. Our extrapolation is justified by the fact that the considered stars because of their surface convection zones are fairly similar to the Sun. The effect of magnetic field strength on the generated wave energy fluxes has been extensively discussed by Musielak, Rosner & Ulmschneider (1989), Musielak et al. (1995) and in Paper I. It has been found that decreasing the field strength of the flux tube increases the amount of the generated wave energy. In this paper, we assume a constant field strength of $B = 0.875 B_{\rm eq}$ for all computations.

2.2 Stellar convection zones

The magnetic flux tubes are embedded in non-magnetized convection zones, which are modelled using the standard stellar envelope code that is based on the mixing-length theory, allowing the calculation of longitudinal tube wave energy fluxes for a large variety of stars of different effective temperature, surface gravity and metal abundances.

More detailed models based on 2D or 3D radiation-hydrodynamic simulations for individual stars have also become available in the literature. The simulations based on such models of stellar convection and mixing-length models show that the maximum convective velocities occur at optical depths of $\tau_{5000} \approx 10$–100. For example, Steffen (1993) found in his time-dependent solar numerical convection calculations that maximum convective velocities $v_{\rm CMax} \approx 2.8$ km s^{-1} are reached at $\tau_{5000} \approx 50$ and that these values can be reproduced by the mixing-length theory with a mixing-length parameter of $\alpha \approx 2$. This choice of $\alpha = 2$ is also consistent with time-dependent hydrodynamic simulations of stellar convection of stars other than the Sun (Trampedach et al. 1997), as well as by a careful fitting of evolutionary tracks of the Sun with its present luminosity, effective temperature and age (Hünsch & Schröder 1997; Schröder & Eggleton 1996).

Additionally, recent state-of-the-art solar convection zone simulations by Stein et al. (2009a,b) encompassing the scale of supergranules concluded that the behaviour of solar convection is consistent with the mixing length of about $\alpha = 1.8$.

From the above, one can conclude that recent simulations are, in principle, consistent with the mixing-length concept (in the case of selected features of convection) and that the wave energy flux is well defined for a given star if the mixing-length parameter α can be specified.

Surely, some principal uncertainties in the value of α remain, which has also been highlighted by previous studies of Nordlund & Dravins (1990) for main-sequence stars other than the Sun. For this reason, the upcoming investigation by Fawzy & Cuntz (2010) will consider a broader range of α values concerning theoretical models of longitudinal flux tube wave energy generation for main-sequence stars.

Finally, I would like to point out that acoustic and magnetic heating models based on the computed wave energy fluxes using the mixing-length concept have been highly successful in explaining the observed Ca II and Mg II emission for both active and inactive stars (e.g. Buchholz, Ulmschneider & Cuntz 1998; Cuntz et al. 1999; Paper I; Fawzy et al. 2002b; Rammacher & Cuntz 2003).

For the choice of the mixing-length parameter α, I decided to keep the same value of $\alpha = 2$ as used in Paper I. The main motivation is to provide consistency (including the possibility of detailed comparisons) with the previous work described in Paper I.

2.3 Magnetic flux tube–convection zone interaction

The main mechanism responsible for generating the longitudinal tube wave energies is the non-linear response of vertically oriented flux tubes to external turbulent motions. The pressure fluctuations produced by turbulent motions squeeze the flux tubes and thus generate wave energies. For the current computations, we follow the approach described by Ulmschneider & Musielak (1998) and in Paper I to model turbulent motions by using an extended Kolmogorov turbulent energy spectrum with a modified Gaussian frequency factor (Musielak et al. 1994). The computations require specifying the rms velocity fluctuations at a squeezing point as given by $u_{\mathrm{t}} = \upsilon_{\mathrm{CMax}}/2$, with υ_{CMax} being the maximum convective velocity (refer to Paper I for the choice of u_{t}). The value of υ_{CMax} is evaluated from the stellar convection zone models based on the mixing-length theory with $\alpha = 2.0$. The computed external pressure fluctuations are then converted into internal gas and magnetic field perturbations by using the horizontal pressure balance equation. The internal pressure fluctuations produce velocity perturbations inside the flux tube which serve as a boundary condition for the time-dependent wave propagation code.

A study performed by Ulmschneider & Musielak (1998) has shown that the location of the squeezing point does not affect the generated wave energy fluxes. Based on this result, we fix the location for all our computed cases to $\tau_{5000} = 1$.

Fig. 1 and Table 1 show the variation of the rms velocity fluctuations u_{t} with metal abundances for the different models used in the current computations.

A modified time-dependent wave code based on an earlier version by Herbold et al. (1985) is then employed to compute the instantaneous and time-averaged longitudinal tube wave energy fluxes at the squeezing height.

The generated wave energy fluxes are a mixture of propagating and non-propagating waves. By use of Fourier transforms, we filter out the propagating waves and calculate the time-averaged wave energy fluxes. The filter is set in the frequency domain at the Defouw cut-off frequency (Defouw 1976). For the computations of stellar model chromospheres, only the upward propagating waves contribute to the heating of outer layers, so we compute the time-averaged upward propagating energy fluxes in addition to the previously computed quantities. Refer to Paper I for more details about the process of removing the non-propagating waves from the generated mixture. The computations are adiabatic and shocks cannot form because our computational domain remains close to the stellar surface.

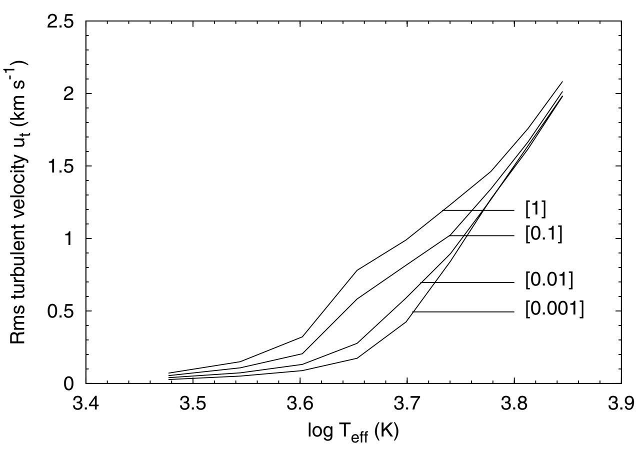

Figure 1. Rms turbulent velocities at the squeezing point ($\tau_{5000} = 1$) for main-sequence stars with $\log g = 4.44$ and for different metal abundances Z_{m} relative to solar (shown in brackets).

Table 1. rms turbulent velocities u_{t} (cm s^{-1}) at the squeezing height in stars with different effective temperatures T_{eff}, gravity $\log g = 4.44$ and relative metal abundances $Z_{\mathrm{m}}/Z_{\mathrm{m0}}$ ranging from 1, 0.1, 0.01, to 0.001.

T_{eff}	[1]	[0.1]	[0.01]	[0.001]
3000	7.1×10^3	5.4×10^3	4.0×10^3	2.7×10^3
3500	1.5×10^4	1.1×10^4	7.3×10^3	5.1×10^3
4000	3.2×10^4	2.1×10^4	1.3×10^4	8.9×10^3
4500	7.8×10^4	5.8×10^4	2.8×10^4	1.7×10^4
5000	9.9×10^4	8.2×10^4	5.9×10^4	4.2×10^4
5500	1.2×10^5	1.0×10^5	8.9×10^4	8.4×10^4
6000	1.5×10^5	1.3×10^5	1.3×10^5	1.3×10^5
6500	1.8×10^5	1.7×10^5	1.6×10^5	1.7×10^5
7000	2.1×10^5	2.0×10^5	2.0×10^5	2.0×10^5

2.4 Non-solar metallicities

The calculations of the external and internal models require opacity tables valid for stars with reduced metal abundances. The results presented in Paper I were based on opacity tables valid for solar chemical abundance. The tables were compiled by Bohn (1984) and Theurer (1993) from different opacity tables given by Alexander (1975, 1989), Cox & Tabor (1976), Yorke (1979, 1980), Meyer-Hofmeister (1982) and Weiss (1990). To account for the non-solar metal abundances we use opacity tables computed with the ATLAS program of Kurucz (1992, 1996). The tables were computed for the following metal abundances: $Z_{\mathrm{m}} = 2\times10^{-2}$, 2×10^{-3}, 2×10^{-4} and 2×10^{-5}. The solar chemical abundance by mass is for hydrogen $X_{\mathrm{m}} = 0.70$, helium $Y_{\mathrm{m}} = 0.28$ and metals $Z_{\mathrm{m0}} = 2 \times 10^{-2}$. The wave energy fluxes computed in this paper are obtained with the Kurucz opacity for the above-mentioned metal abundances.

The range of validity of these opacity tables is discussed in detail by Ulmschneider et al. (1999). The used opacity tables have limited ranges in the values of opacities for cool stars and upper limits for the high temperature and densities; for this reason we consider only stars with effective temperatures in the range $3000 \le T_{\mathrm{eff}} \le 7000$ K and $\log g = 4.44$.

3 RESULTS AND DISCUSSION

3.1 Wave energy power spectra and propagating wave fluxes

Wave flux power spectra have been computed for each combination of effective temperature T_{eff} and metallicity for flux tubes with magnetic field strength $B = 0.875B_{\mathrm{eq}}$ embedded in the atmosphere of main-sequence stars with $\log g = 4.44$. We applied a high-pass filter at the Defouw cut-off frequency, ω_{D}, on the velocity and pressure fluctuations inside the flux tube to separate the propagating waves. The position of the filter is shown by the low-frequency cut-off in Fig. 2. The Defouw cut-off frequencies do not depend on the metal

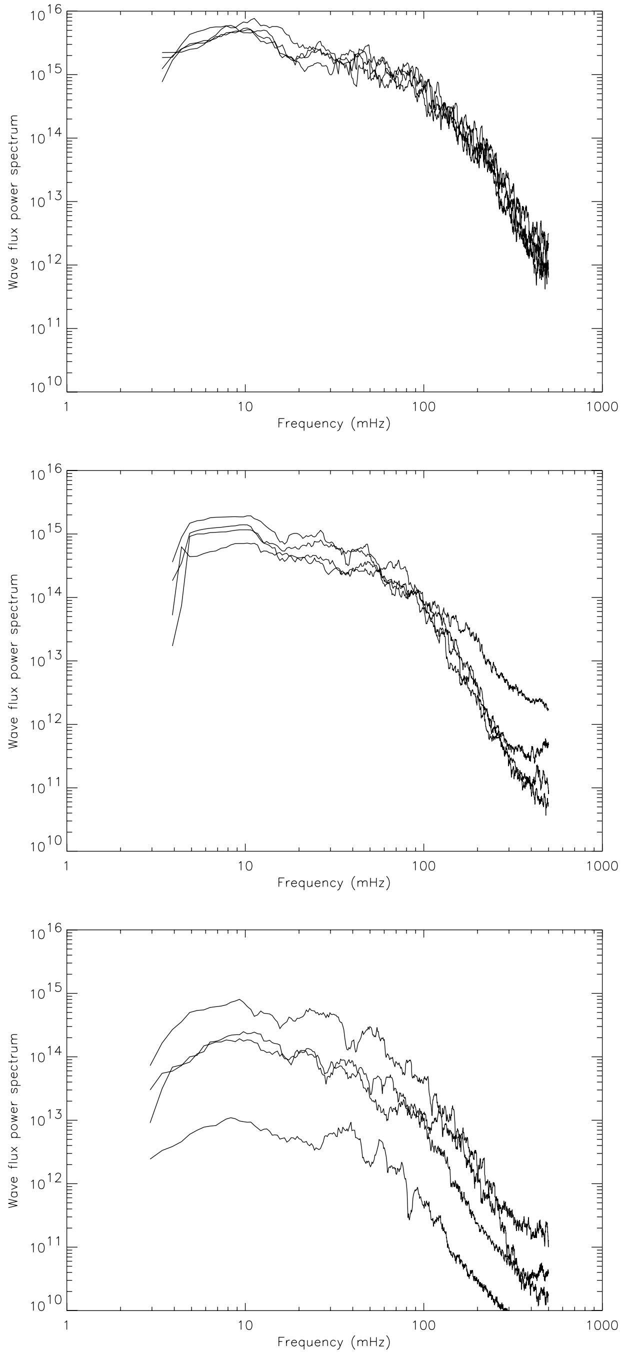

Figure 2. Power spectra of the wave energy fluxes in flux tubes embedded in the atmospheres of main-sequence stars with effective temperatures $T_{\rm eff} = 6500$ K (top panel), $T_{\rm eff} = 5500$ K (middle panel) and $T_{\rm eff} = 5000$ K (bottom panel) and $\log g = 4.44$. For a given effective temperature, the four power spectra represent metallicity ranging from $Z_{\rm m}/Z_{\rm m0} = 1$ (highest) to $Z_{\rm m}/Z_{\rm m0} = 0.001$ (lowest). The power spectrum is shown as a function of circular frequency ω.

abundance. The power spectrum reaches their maxima at roughly $2\omega_{\rm D}$ and decreases towards higher frequencies. To show the effect of metallicity on the power spectrum of the propagating waves, we present in Fig. 2 three cases for main-sequence stars of effective temperatures $T_{\rm eff} = 6500$, 5500 and 5000 K, with metallicities ranging from $Z_{\rm m}/Z_{\rm m0} = 1$ to 0.001.

It can be seen that the power spectra for hot stars (top panel) are almost the same and there is essentially no variation for the different metallicities. This very little dependence is mainly due to the fact that opacity in hot stars is mainly due to hydrogen and less affected by changes in metal abundance. The behaviour is different for cool stars (bottom panel) which show a strong metallicity dependence. Here the wave flux power decreases with decreasing metallicity. This can be explained by the fact that for cool stars the opacity is mainly due to metals and thus enhances this dependence. The stars in the middle panel show an intermediate behaviour. There is a clear decrease in the wave power with decreasing metallicity for stars with effective temperatures $T_{\rm eff} < 5500$ K. This can be explained by the fact that by lowering the metallicity, the squeezing point will be in deeper layers where the rms turbulent velocity is smaller and thus the efficiency to generate longitudinal tube waves decreases.

As shown in Paper I, the high frequencies in the power spectrum are due to the stochastic nature and the spikiness of the wave generation process. The generated wave power spectra for stars with different metallicities have the same shape as those computed for stars with solar metal abundances (see fig. 12 of Paper I).

3.2 Time-averaged upward wave energy fluxes

For the evaluation of reliable time-averaged wave energy fluxes and due to the spiky nature of the instantaneous wave energy fluxes, the wave propagation code has to be run over a time of about $35P_{\rm D}$, with $P_{\rm D}$ being the wave period of the Defouw cut-off frequency. In addition to the total (propagating and non-propagating) wave energy fluxes, we have computed the time-averaged upward propagating wave energy fluxes for different combinations of $T_{\rm eff}$ and $Z_{\rm m}$ and $\log g = 4.44$. The results are listed in Table 2.

The amount of wave energy for a given metallicity depends strongly on the stellar effective temperature. The time-averaged upward propagating wave energy flux increases with increasing $T_{\rm eff}$. A decrease in effective temperature from $T_{\rm eff} = 7000$ to 3000 K reduces the time-averaged upward propagating energy fluxes by factors of 3.0×10^3, 3.5×10^3, 3.5×10^3 and 1.1×10^4 for $Z_{\rm m}/Z_{\rm m0} = 1$, 0.1, 0.01 and 0.001, respectively. This large difference in the generated energies can be explained by the difference in convective velocities between hot and cool stars; for hot stars the turbulent eddies have much higher velocities which enhance the efficiency of generating waves at the squeezing point.

The efficiency of tube wave generation is found to depend strongly on the rms turbulent velocities $u_{\rm t}$ and thus lowering of $u_{\rm t}$ decreases the generated wave energy fluxes. As shown in Fig. 1 and Table 1, for a given value of $Z_{\rm m}$ and $\log g = 4.44$ the values of $u_{\rm t}$ are strongly affected by $T_{\rm eff}$: decreasing the effective temperature by 500 K reduces the values of $u_{\rm t}$ roughly by a factor of 2 for stars with $T_{\rm eff} \le 4500$ K. For hotter stars $T_{\rm eff} \ge 5000$ K, the values of $u_{\rm t}$ decrease roughly by a factor of 0.2.

The dependence of the generated upward propagating wave energy fluxes on $u_{\rm t}$ for stars with different metal abundances can be approximately fitted by $\log F = A(\log u_{\rm t})^B$. The coefficients of the fits for four different values of metal abundance are given in Table 3.

It is important to mention here the result obtained in Paper I that the dependence of the generated wave energy fluxes on the magnetic field strength in the flux tube does not change much when stars of different $T_{\rm eff}$ and similar gravities are considered, which is the case for the considered main-sequence stars with $\log g = 4.44$.

Table 2. Time-averaged upward propagating energy fluxes in stars with different effective temperatures $T_{\rm eff}$, gravity $\log g = 4.44$ and metal abundances ranging from $Z_{\rm m}/Z_{\rm m0} = 1$ to 0.001.

$T_{\rm eff}$	[1]	[0.1]	[0.01]	[0.001]
3000	2.5×10^5	2.1×10^5	1.8×10^5	6.0×10^4
3500	5.3×10^5	4.2×10^5	2.4×10^5	1.5×10^5
4000	3.5×10^6	2.6×10^6	8.8×10^5	3.2×10^5
4500	8.3×10^7	9.3×10^7	4.8×10^6	3.7×10^6
5000	1.4×10^8	2.3×10^8	1.0×10^8	2.9×10^7
5500	3.2×10^8	2.5×10^8	3.3×10^8	3.1×10^8
6000	3.8×10^8	5.4×10^8	4.1×10^8	4.2×10^8
6500	5.9×10^8	7.5×10^8	6.7×10^8	5.9×10^8
7000	7.5×10^8	7.3×10^8	6.3×10^8	6.6×10^8

Table 3. Coefficients of the fits $\log F = A\,(\log u_{\rm t})^B$ for main-sequence stars with $\log g = 4.44$ and different values of metallicity $Z_{\rm m}/Z_{\rm m0}$.

$Z_{\rm m}/Z_{\rm m0}$	A	B
1.0	0.505 ± 0.070	1.724 ± 0.087
0.1	0.628 ± 0.098	1.606 ± 0.098
0.01	0.692 ± 0.112	1.544 ± 0.103
0.001	0.718 ± 0.086	1.522 ± 0.077

3.3 Dependence on metal abundances

According to the results presented in Figs 3 and 4, there are two main regions of different dependence of the generated wave energy fluxes on metallicity. The two regions are divided by stars of effective temperature $T_{\rm eff} = 5500$ K.

Hot stars with $T_{\rm eff} \geq 5500$ K and higher convective velocities have relatively high longitudinal wave energy fluxes that show very little change with the metal abundance, as shown in Fig. 3 for the mixture of propagating and non-propagating waves and in Fig. 4 for only upward propagating waves. This can be explained by the fact that for hot stars, the opacity is mainly due to hydrogen. For cool stars, where the opacity is mainly due to metals, a strong dependence on metallicity is found.

For cool stars with $T_{\rm eff} < 5500$ K, lowering the metal abundance strongly reduces the amount of the wave energy flux. It is clearly notable that a decrease in metallicity by an order of magnitude from $Z_{\rm m}/Z_{\rm m0} = 0.1$ to 0.01 reduces the wave energy fluxes by a factor of up to 10 for stars with $T_{\rm eff} = 4500$ K and $\log g = 4.44$. This factor drops to about 2 for other stars.

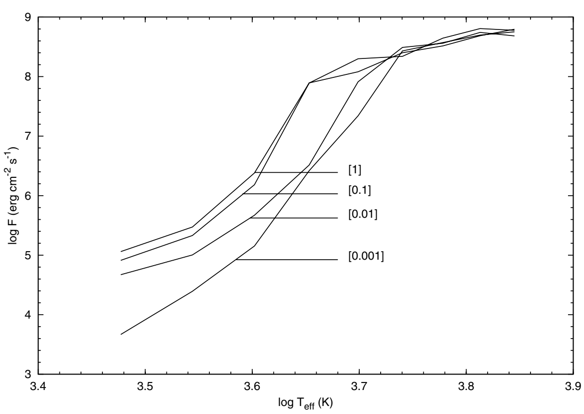

Figure 3. Time-averaged wave energy fluxes for main-sequence stars: the magnetic flux tubes with field strength $B = 0.875B_{\rm eq}$ at height $z = 0$ for a star with surface gravity $\log g = 4.44$ and effective temperatures ranging from $T_{\rm eff} = 3000$ to 7000 K. The metal abundances range from $Z_{\rm m}/Z_{\rm m0} = 1$ to 0.001.

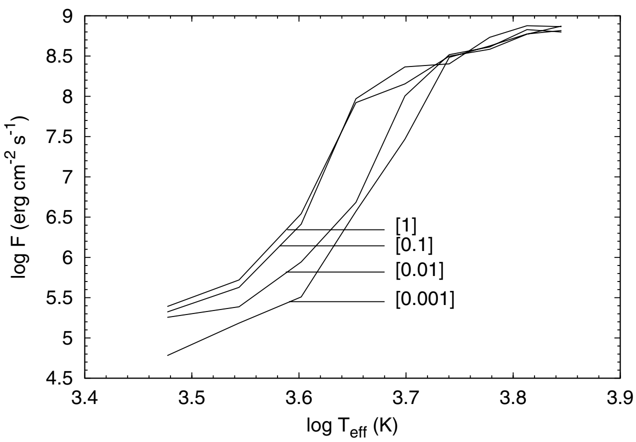

Figure 4. Same as Fig. 3, but for upward propagating waves.

The maximum wave energy flux generated in stars with low metallicities is 7.5×10^8 erg cm^{-2} s^{-1} which is met for a star of $T_{\rm eff} = 7000$ K, and it is practically independent of metallicity.

3.4 Comparison to linear results

A comparison between the analytical results obtained by Musielak et al. (2002) shows that the current results are higher than those obtained by the analytical method for the same stars. These differences vary as a function of effective temperature.

As shown in Table 4, the average ratios between the current results and the numerical results obtained by Musielak et al. (2002) are about 2000, 60, 4 for $T_{\rm eff} = 3000$, 5000, 7000 K, respectively. This difference can be explained by the fact that the analytical treatment does not allow for non-linear waves with large amplitudes. The

Table 4. A comparison between the wave energy fluxes for upward propagating longitudinal tube waves in stars with gravity $\log g = 4.44$ obtained analytically and numerically.

$T_{\rm eff}$	$F_{\rm A}$	$F_{\rm N}$
Metallicity ($Z_{\rm m}/Z_{\rm m0} = 0.1$)		
3000	4.8×10^2	2.1×10^5
5000	4.9×10^6	2.3×10^8
7000	1.7×10^8	7.3×10^8
Metallicity ($Z_{\rm m}/Z_{\rm m0} = 0.01$)		
3000	1.0×10^2	1.8×10^5
5000	2.9×10^6	1.0×10^8
7000	1.7×10^8	6.3×10^8
Metallicity ($Z_{\rm m}/Z_{\rm m0} = 0.001$)		
3000	2.0×10^1	6.0×10^4
5000	2.7×10^5	2.9×10^7
7000	1.6×10^8	6.6×10^8

Note: The second column shows the analytical results and the third column shows the corresponding numerical results.

non-linear effects enhance the obtained values. A comparison with the results obtained by Ulmschneider et al. (1999) for the acoustic wave energy fluxes shows a similar dependence on metallicity for cool stars.

3.5 Comparison to observational data

Earlier studies by Schrijver (1987) and Rutten et al. (1991) have not identified a metallicity effect on chromospheric emission, particularly Ca II and Mg II, especially in main-sequence stars. On the other hand, more recent observations by the *Hubble Space Telescope* concerning chromospheric Mg II fluxes given by Dupree, Li & Smith (2007) indicate signs of dependence on metallicity at the lowest metallicities, although these results were obtained for giants rather than dwarfs.

It is important to note that a comparison of such data with the obtained results in the current study should be viewed with extreme caution. The current results of the longitudinal tube wave fluxes are generated in the vicinity of $\tau_{5000} = 1$ and are therefore relevant in layers beyond the formation heights of Ca II and Mg II emission fluxes. These generated wave fluxes also dissipate part of their energies while propagating upwards in the stellar atmosphere by forming shocks.

Any chromosphere-type metallicity effect in stars of different levels of magnetic activity is in competition with other processes or phenomena such as the relatively poorly known value of $B/B_{\rm eq}$ (or a statistical distribution of that value in the framework of more sophisticated models), the magnetic filling factor and wave propagation effects (note that the place where the longitudinal tube wave flux emerges is not identical to where the Ca II/Mg II lines form). Furthermore, in realistic heating scenarios, there is also a need to also consider competing heating mechanisms (i.e. processes other than longitudinal tube waves; see review by Narain & Ulmschneider 1996).

For these reasons, the present study is intended to be a purely theoretical study; it is meant to be a resource study for future modelling efforts.

4 CONCLUSIONS

We have computed the longitudinal wave energy fluxes generated at the base of stellar magnetic flux tubes with non-solar metal abundances. It is important to mention here that the obtained wave energy fluxes are for stars that have solar-like structure, activity and small magnetic filling factors similar to the Sun (e.g. de Wijn et al. 2009). The results are valid for a single flux tube based on the four independent parameters: effective temperature $T_{\rm eff}$, gravity g, metal abundance $Z_{\rm m}$ and the magnetic field strength B at the stellar surface. From the obtained results we draw the following conclusions.

(i) The effect of metallicity is very important for cool stars, with effective temperatures $T_{\rm eff} < 5500$ K and $\log g = 4.44$.

(ii) The shapes of the generated wave energy spectra in stars with non-solar metal abundance are similar to stars with similar $T_{\rm eff}$, gravity g and solar metal abundance.

(iii) For hot stars with $T_{\rm eff} > 5500$ K, the generated wave energy fluxes show no notable dependence on metallicity.

(iv) A decrease in metallicity by an order of magnitude from $Z_{\rm m}/Z_{\rm m0} = 0.1$ to 0.01 reduces the wave energy fluxes by a factor of up to 10 for stars with $T_{\rm eff} = 4500$ K and $\log g = 4.44$. This factor drops to about 2 for other stars.

(v) The maximum obtained wave energy flux for low-metallicity stars is about 7.3×10^8 erg cm^{-2} s^{-1}.

(vi) Comparing the current results to those obtained by Musielak et al. (2002) for linear waves shows that the wave energy fluxes are much higher by factors ranging between 2000, 60 and 4 for $T_{\rm eff} =$ 3000, 5000 and 7000 K, respectively.

(vii) The effect of metallicity on the generation of magnetic and non-magnetic waves is found to be similar.

(viii) The obtained wave energy fluxes are essential for constructing theoretical models for the magnetic chromospheres of low-metallicity stars.

ACKNOWLEDGMENTS

I would like to thank Professor Dr P. Ulmschneider, Professor Dr Z. E. Musielak, Dr M. Cuntz and Professor Dr K. Stępień for invaluable discussions and comments. I also thank the anonymous referee for valuable comments. This work was supported in part by the Izmir University of Economics.

REFERENCES

Alexander D. R., 1975, ApJS, 29, 363
Alexander D. R., 1989, ApJ, 345, 1014
Bohn H. U., 1984, A&A, 136, 338
Buchholz B., Ulmschneider P., Cuntz M., 1998, ApJ, 494, 700
Cox A. N., Tabor J. E., 1976, ApJS, 31, 271
Cuntz M., Rammacher W., Ulmschneider P., Musielak Z. E., Saar S. H., 1999, ApJ, 522, 1053
Defouw R. J., 1976, ApJ, 209, 266
de Wijn A. G., Stenflo J. O., Solanki S. K., Tsuneta S., 2009, Space Sci. Rev., 144, 275
Dupree A. K., Li T. Q., Smith G. H., 2007, ApJ, 134, 1348
Fawzy D., Cuntz M., 2010, A&A, submitted
Fawzy D., Rammacher W., Ulmschneider P., Musielak Z. E., Stępień K., 2002a, A&A, 386, 971
Fawzy D., Ulmschneider P., Stępień K., Musielak Z. E., Rammacher W., 2002b, A&A, 386, 983
Fawzy D., Stępień K., Ulmschneider P., Rammacher W., Musielak Z. E., 2002c, A&A, 386, 994
Kurucz R. L., 1992, in Barbuy B., Renzini A., eds, Proc. IAU Symp. 149, The Stellar Population of Galaxies. Kluwer, Dordrecht, p. 225
Kurucz R. L., 1996, in Adelman S. J., Kupta F., Weiss W., eds, ASP Conf. Ser. Vol. 108, Workshop on Model Atmospheres and Spectrum Synthesis. Astron. Soc. Pac., San Francisco, p. 2
Hassan S. S., Kalkofen W., van Ballegooijen A. A., Ulmschneider P., 2003, ApJ, 585, 1138
Herbold G., Ulmschneider P., Spruit H. C., Rosner R., 1985, A&A, 145, 157
Huang P., Musielak Z. E., Ulmschneider P., 1995, A&A, 279, 579
Hünsch M., Schröder K. P., 1997, A&A, 309, L51
Meyer-Hofmeister E., 1982, in Schaifers K., Voigt H. H., eds, Stellar Structure and Evolution. Springer, Berlin, p. 152
Musielak Z. E., Rosner R., Ulmschneider P., 1989, ApJ, 337, 470
Musielak Z. E., Rosner R., Stein R. F., Ulmschneider P., 1994, ApJ, 423, 474
Musielak Z. E., Rosner R., Gail H. P., Ulmschneider P., 1995, ApJ, 448, 865
Musielak Z. E., Rosner R., Ulmschneider P., 2002, ApJ, 573, 418
Narain U., Ulmschneider P., 1996, Space Sci. Rev., 75, 453
Nordlund A., Dravins D., 1990, A&A, 228, 155
Rammacher W., Cuntz M., 2003, ApJ, 594, L51
Rutten R. G. M., Schrijver C. J., Lemmens A. F. P., Zwaan C., 1991, A&A, 252, 203
Schrijver C. J., 1987, A&A, 172, 111

Schröder K. P., Eggleton P. P., 1996, Rev. Modern Astron., 9, 221
Solanki S. K., 1993, Space Sci. Rev., 63, 1
Steffen M., 1993, Habil. thesis, Univ. Kiel
Stein R. F., Nordlund Å., Georgobiani D., Benson D., Schafenberger W., 2009a, in Dikpati M., Gonzalez-Hernandez I., Arentoft T., Hill F., eds, ASP Conf. Ser., Solar–Stellar Dynamos as Revealed by Helio- and Asteroseismology, GONG 2008/SOHO XXI Meeting. Astron. Soc. Pac., San Francisco, p. 421
Stein R. F., Georgobiani D., Schafenberger W., Nordlund Å., Benson D., 2009b, in Stempels E., ed., AIP Conf. Proc. Vol. 1094, Cool Stars, Stellar Systems, and the Sun 15. Am. Inst. Phys., New York, p. 764
Stenflo J. O., 1978, Rep. Progress Phys., 75, 3
Theurer J., 1993, Diploma thesis, Univ. Heidelberg
Trampedach R., Christensen-Dalsgaard J., Nordlund A., Stein R. F., 1997, in Pijpers F. P., Christensen-Dalsgaard J., Rosenthal C. S., eds, Solar Convection and Oscillations and their Relationship. Kluwer, Dordrecht, p. 73
Ulmschneider P., Musielak Z. E., 1998, A&A, 338, 311
Ulmschneider P., Theurer J., Musielak Z. E., 1996, A&A, 315, 212
Ulmschneider P., Theurer J., Musielak Z. E., Kurucz R., 1999, A&A, 347, 243
Ulmschneider P., Musielak Z. E., Fawzy D. E., 2001, A&A, 374, 662 (Paper I)
Vernazza J. E., Avrett E. H., Loeser R., 1981, ApJS, 45, 635
Weiss A., 1990, At. Data Nucl. Data Tables, 45, 209
Yorke H. W., 1979, A&A, 80, 308
Yorke H. W., 1980, A&A, 85, 215

This paper has been typeset from a TEX/LATEX file prepared by the author.